

Connecting Infrared Surface Brightness Fluctuation Distances to Type Ia Supernova Hosts: Testing the Top Rung of the Distance Ladder

PETER GARNAVICH,¹ CHARLOTTE M. WOOD,¹ PETER MILNE,² JOSEPH B. JENSEN,³ JOHN P. BLAKESLEE,⁴
PETER J. BROWN,^{5,6} DANIEL SCOLNIC,⁷ BENJAMIN ROSE,⁷ AND DILLON BROUT^{8,9}

¹University of Notre Dame, Department of Physics and Astronomy, 225 Nieuwland Science Hall, Notre Dame, IN 46556

²University of Arizona, Steward Observatory, 933 N. Cherry Avenue, Tucson, AZ 85721, USA

³Utah Valley University, Department of Physics, 800 W. University Parkway, MS 179, Orem, UT 84058, USA

⁴NSF's NOIRLab, 950 N. Cherry Ave., Tucson, AZ 85719, USA

⁵Department of Physics and Astronomy, Texas A&M University, 4242 TAMU, College Station, TX 77843, USA

⁶George P. and Cynthia Woods Mitchell Institute for Fundamental Physics & Astronomy, College Station, TX 77843, USA

⁷Duke University, Department of Physics, 120 Science Drive, Durham, NC, 27708 USA

⁸Center for Astrophysics, Harvard & Smithsonian, 60 Garden Street, Cambridge, MA 02138, USA

⁹NASA Einstein Fellow

ABSTRACT

We compare infrared surface brightness fluctuation (IR SBF) distances measured in galaxies that have hosted type Ia supernovae (SNe Ia) to distances estimated from SNe Ia light curve fits. We show that the properties of SNe Ia found in IR-SBF hosts are very different from those exploding in Cepheid calibrators, therefore, this is a direct test of systematic uncertainties on estimation of the Hubble constant (H_0) using supernovae. The IR SBF results from [Jensen et al. \(2021\)](#) provide a large and uniformly measured sample of IR SBF distances which we directly compare with distances to 25 SNe Ia host galaxies. We divide the Hubble flow SNe Ia into sub-samples that best match the divergent supernova properties seen in the IR SBF hosts and Cepheid hosts. We further divide the SNe Ia into a sample with light curve widths and host masses that are congruent to those found in the SBF-calibrated hosts. We refit the light curve stretch and color correlations with luminosity, and use these revised parameters to calibrate the Hubble flow SNe Ia with IR SBF calibrators. Relative to the Hubble flow, the average calibrator distance moduli vary by 0.03 mag depending on the SNe Ia subsamples examined and this adds a 1.8% systematic uncertainty to our Hubble constant estimate. Based on the IR SBF calibrators, $H_0 = 74.6 \pm 0.9(\text{stat}) \pm 2.7(\text{syst}) \text{ km s}^{-1} \text{ Mpc}^{-1}$, which is consistent with the Hubble constant derived from SNe Ia calibrated from Cepheid variables. We conclude that IR SBF provides reliable calibration of SNe Ia with a precision comparable to Cepheid calibrators, and with a significant saving in telescope time.

Keywords: Supernovae; Cosmological Parameters; Hubble Constant; Distance Indicators - Surface Brightness Fluctuations

1. INTRODUCTION

The precise determination of the present expansion rate of the universe, the Hubble constant (H_0), is a fundamental goal of modern cosmology ([Lemaître 1927](#); [Hubble 1929](#); [Huchra 1992](#); [Hamuy et al. 2021](#)). H_0 can be estimated using “local” distance indicators, such as type Ia supernovae (SNe Ia), and predicted from the standard Λ CDM model calibrated with early-universe indicators, such as the cosmic microwave background (CMB). However, the values of H_0 determined from local and early-universe indicators are significantly discrepant ([Riess et al. 2022](#); [Planck Collaboration et al.](#)

[2020](#)). This “tension” in the value of H_0 could indicate new physics yet to be discovered, or could be a result of unaccounted observational uncertainties (e.g. [Bernal et al. 2016](#); [Efstathiou 2021](#)), or both.

SNe Ia are excellent distance indicators for cosmology. Their extreme luminosities allow them to be observable out to high redshifts and their predictable light curves make these supernovae useful as a standardizable candles. To date, SNe Ia have been used to constrain the mass density of the universe ([Perlmutter et al. 1998](#); [Garnavich et al. 1998](#)), reveal the cosmic acceleration and dark energy ([Riess et al. 1998](#); [Perlmutter et al.](#)

1999), and they continue to provide a tool for narrowing the uncertainty on H_0 (Freedman et al. 2001; Riess et al. 2009, 2019, 2022).

With significant variations in their peak luminosity, SNe Ia are clearly not standard candles. However, empirical correlations between luminosity, color (Riess et al. 1996), and light curve shape (Phillips 1993) mean that SNe Ia are standardizable candles. SNe Ia properties are also found to correlate with host-galaxy type, with brighter, slower-declining SNe Ia typically occurring in spiral galaxies and dimmer, faster-declining SNe Ia typically occurring in elliptical galaxies (Hamuy et al. 1995; Gallagher et al. 2005; Sullivan et al. 2006; Pruzhinskaya et al. 2020). Surprisingly, the mass of a host galaxy is found to correlate with distance residuals after standardization (Kelly et al. 2010; Lampeitl et al. 2010; Sullivan et al. 2010).

To estimate H_0 , the luminosity of SNe Ia must be calibrated using locally abundant distance indicators, such as Cepheid variable stars, tip-of-the-red-giant-branch (TRGB) stars (Freedman et al. 2019), or surface brightness fluctuations (SBF) (Tonry & Schneider 1988; Blakeslee et al. 2009). In turn, the luminosities of these objects must be calibrated by local techniques and these steps in distance form the basis of the “distance ladder” needed to reach the smooth Hubble flow. Much of the current uncertainty in H_0 as determined by SNe Ia comes from the statistical and systematic errors that accumulate from the lower rungs in the cosmic distance ladder. In particular, Cepheid variable stars have provided a sturdy intermediate step for the SNe Ia distance calibration, but testing for their systematic uncertainties is critical to assure the reliability of cosmological studies.

SNe Ia distances can instead be calibrated using TRGB or SBF in an effort to check for the systematic errors in the H_0 estimation. SBF is a particularly interesting calibration method as it provides several advantages over Cepheid measurements. SBF does not require resolving individual stars, and can therefore be applied out to about 100 Mpc while maintaining a 5% precision. In comparison, Cepheid calibrators must be within about 40 Mpc to obtain reliable measurements. Further, IR SBF measurements require only 1 to 2 Hubble Space Telescope (*HST*) orbits per galaxy (Jensen et al. 2021) to achieve a 5% distance precision. This can be compared with the more than 1000 total *HST* orbits needed to calibrate 42 SNe Ia hosts using Cepheid variables (Riess et al. 2022). Finally, the SBF method is best applied to elliptical galaxies and therefore targets a complementary population of galaxies and SNe Ia than Cepheids, which typically occur in spiral galaxies.

The application of SBF to cosmologically interesting distances was demonstrated by Jensen et al. (2001) using space-based, near-infrared (IR) imaging. Most recently, *HST*’s Wide Field Camera 3 (WFC3) has proven to be a superb instrument for SBF distance calibrations, allowing for a median 3.9% distance uncertainty on 63 massive elliptical galaxy distances out to 100 Mpc (Jensen et al. 2021).

From IR SBF distances alone (no SNe Ia), Blakeslee et al. (2021) provided a robust measurement of $H_0 = 73.3 \pm 0.7(\text{stat}) \pm 2.5(\text{syst}) \text{ km s}^{-1} \text{ Mpc}^{-1}$ based on a combination of Cepheid and TRGB zero-points. Khetan et al. (2021) made an estimate of H_0 by calibrating SNe Ia luminosities from previously published SBF distances compiled from literature sources. However, their result had significant statistical uncertainties that did not strongly constrain H_0 , and this was primarily due to the inclusion of SBF distances acquired from heterogeneous sources.

In this paper, we compare the consistent set of IR SBF distances derived from *HST* imaging of 25 unique SNe Ia host galaxies (Jensen et al. 2021) with a consistent set of SNe Ia light curve distances from SALT2 (Scolnic et al. 2022). Since these SBF distances are calibrated to the Cepheid zero-point, we are still tied to the systematic uncertainties connected to the lower rungs of the distance ladder. Our primary goal is to test for significant systematic differences when calibrating SNe Ia in the Hubble flow using IR SBF distances versus Cepheid distances, given that the two methods target different host-galaxy types. We also test the quality of the IR SBF distance measurement uncertainties by comparing them directly to the well-determined scatter in the SNe Ia luminosities.

The approach taken in this analysis can be considered a ‘Four-Rung Distance Ladder’. While Three-Rung Distance Ladders have received more attention (e.g. Freedman et al. 2019; Riess et al. 2022), our approach is able to address possible systematic limitations of the three-rung method. To summarize, Freedman et al. (2019) and Riess et al. (2022) tie geometric distance probes to stellar probes (TRGB and Cepheid respectively), then these stellar probes to supernova probes, and finally supernova probes to redshifts in order to measure the Hubble constant. Within these three rungs, various choices can be made. In Riess et al. (2022), the SNe Ia in the second rung and third rung are just from star-forming galaxies and taken from the Pantheon+ compilation; in Freedman et al. (2019), the SNe Ia for the second rung are taken from the literature and the third rung is taken solely from the CSP sample. A separate three-rung approach is done by Blakeslee et al. (2021), which use SBF

in the role of SNe Ia. In this approach, either Cepheids or TRGB can be used in the first and second rung. Our four-rung approach, which allows the usage of a different sample of SNe Ia, is most similar to Khetan et al. (2021); this analysis ties geometry to Cepheids, Cepheids to literature SBF, literature SBF to literature SNe Ia, and finally literature SNe Ia to more distant literature SNe Ia in the Hubble Flow. In our analysis, we use a single sample of homogeneously calibrated IR SBF distances (Jensen et al. 2021), and a homogeneously calibrated set of SNe Ia distances (Brout et al. 2022). While we use Cepheids in our first rung, Blakeslee et al. (2021) has shown that combining TRGB and Cepheids changes the resulting value of H_0 by only 0.1%.

A direct comparison of the Cepheid and IR SBF distance calibrations is limited by the large peculiar velocities found at the calibrator redshifts of $z < 0.02$. Here, we use the large number of Hubble flow SNe Ia now available in the Pantheon+ recalibration (Scolnic et al. 2022; Brout et al. 2022) as a 0.01 mag precision anchor to the nearby host galaxies. We then compare the scatter and the systematics of Cepheid-calibrated SNe Ia with those of the SBF-calibrated SNe Ia without the need for peculiar velocity models.

A detailed description of our SBF distance and SNe Ia light curve data is given in § 2. Our analysis and comparisons are described in § 3, followed by our H_0 results in § 4 and discussion in § 5. A summary of our conclusions is presented in § 6.

2. DATA

2.1. SBF Distances

Imaging of SNe Ia host galaxies was obtained with the Hubble Space Telescope (*HST*) using the IR channel of the Wide Field Camera 3 (*WFC3*) (PropIDs: 11691, PI Goudfrooij; 11712 & 14219, PI Blakeslee; 14654, PI Milne; 15265, PI Blakeslee). The process of measuring the IR SBF and transforming them to distances is described by Jensen et al. (2015, 2021).

The IR SBF distances were calibrated with optical SBF distances to 16 Fornax and Virgo cluster galaxies (Jensen et al. 2015; Cantiello et al. 2018), which are based on the Cepheid zero points (Blakeslee et al. 2009, 2021). A discussion of the of the SBF calibration to the Cepheid zero-point is given in Appendix A of Blakeslee et al. (2010). The IR SBF distance moduli have been corrected to the improved LMC distance by shifting -0.023 mag (Pietrzyński et al. 2019). We use the Blakeslee et al. (2021) estimate of the zero-point uncertainty in our total error budget (see Section 4.4).

IR SBF distances to Fornax cluster members were not included in Jensen et al. (2021). For consistency, the dis-

tances from WFC3/IR images (NGC1316, GO 13691; NGC1380 & NGC1404, GO 11712) are estimated here using the same methods as described in Jensen et al. (2021) and presented in Table 1. For NGC1380 and NGC1404, the differences between the ACS measurements (Blakeslee et al. 2009) and these WFC3/IR estimates fall within two standard deviations (2σ) of the combined uncertainties.

Measurements of NGC1316, the host of multiple SNe Ia, are problematic. The difference in SBF distances between the ACS and WFC3/IR is more than 3σ . The IR SBF distance to NGC1316 is significantly shorter than the other Fornax galaxies. The origin of this discrepancy is not clear, and we refer the reader to the detailed study by Cantiello et al. (2013) that analyzes the various distance indicators applied to NGC1316.

It is important to note that the IR SBF distances used here are tied to the Cepheid zeropoint in the LMC, Virgo, and Fornax clusters. Thus, these results are not a completely independent measurement of the Hubble constant. However, early-type hosts and their supernova properties are quite different than supernovae calibrated with Cepheids, and this may result in a systematic H_0 offset between the two methods when extended out to the Hubble flow. To test for systematic offsets, we compared the calibrator samples with a large set of Hubble Flow SNe Ia to search for a magnitude shift that is sample dependent. An IR SBF calibration of SNe Ia that is completely independent of Cepheids will require further direct geometrical and TRGB distances to nearby elliptical galaxies out to the distance of the Virgo and Fornax clusters.

2.2. Supernova Light Curves

Empirically, SNe Ia luminosities correlate with the rate of fading after maximum brightness (Phillips 1993) and their color near maximum (Riess et al. 1996). Host galaxy properties, such as total stellar mass, also show some correlation with SNe Ia brightness after correcting for light curve shape and peak color (Kelly et al. 2010).

There have been several light curve “fitters” developed since the original luminosity-light curve shape relation was identified including $\Delta m_{15}(B)$ (Hamuy et al. 1996), MLCS (Riess et al. 1996), MLCS2k2 (Jha et al. 2007), SALT (Guy et al. 2005), and SNooPy (Burns et al. 2011). The Spectral Adaptive Light Curve Template-2 (SALT2; Guy et al. 2007) is an improvement on the original SALT algorithm and has been recently revised (e.g. Taylor et al. 2021).

SALT2 is an empirical model of the spectral evolution of SNe Ia. The model is trained using a large set of supernova spectra and light curves that define a

Table 1. IR SBF Distances to Fornax Hosts

Galaxy	μ (ACS) ^a (mag)	μ (WFC3/IR) ^b (mag)	difference/ σ	hosted SN	Notes
NGC1380	31.609±0.075	31.465±0.075	1.36	92A	
NGC1404	31.503±0.072	31.453±0.084	0.45	07on, 11iv	
NGC1316	31.583±0.065	31.200±0.093	3.37	80N,81D,06dd,06mr	dusty

^aDistance moduli from [Blakeslee et al. \(2009\)](#) corrected by -0.023 mag for revised LMC distance.

^bIR SBF distance moduli using the analysis described in [Jensen et al. \(2021\)](#)

“surface” in wavelength, phase and, flux ([Mosher et al. 2014](#)). The surface is a time-varying spectral energy distribution (SED) that is convolved with redshifted filter transmission functions to generate photometric models. The model photometry is used to fit observed SNe Ia light curves and extract stretch $x1$, color c , and peak magnitude, m_B estimates. These parameters represent the best fit model of the rest-frame light curve observed in a standard B filter. SNe Ia luminosities are corrected to a fiducial light curve through a stretch correlation, α , and a color correlation, β ([Tripp 1998](#)). This form of SNIa distance estimation is often called the Tripp Relation. The SNe Ia distance modulus, μ , is then

$$\mu = m_B + \alpha x1 - \beta c - M_B - \delta_{bias} \quad (1)$$

where m_B is a parameter that represents the observed peak magnitude of the SNe Ia and M_B is the absolute peak magnitude of the fiducial light curve defined at $x1 = 0$ and $c = 0$. The final term, δ_{bias} , is a multi-dimensional bias correction based on SNANA simulations and it is described by [Scolnic et al. \(2022\)](#).

We used the publicly available SNe Ia light curve data described by [Scolnic et al. \(2022\)](#) and [Brout et al. \(2022, e.g. Pantheon+\)](#) that employed a retrained SALT2 algorithm. Distances are based on bias corrections estimated using simulations implemented through the SNANA software package ([Kessler et al. 2009](#)).

When stepping up the distance ladder, H_0 is estimated by calibrating M_B , the peak absolute magnitude of a bias-corrected supernova with normal stretch and color. This is done by estimating the distance to nearby SNe Ia host galaxies using local distance indicators such as Cepheids, TRGB, SBF, and others. The average value of M_B derived from these calibrators is then applied to SNe Ia out in the Hubble flow where peculiar velocities are small compared with the expansion velocity. A difference in this paper, is that we work with distance moduli directly. This is convenient because the SALT2 fitter delivers a distance modulus, μ , for each light curve and

the calibrator distances are provided as distance moduli (e.g. [Jensen et al. 2021](#)). Consequences of this parameterization are discussed in Section 3.4.

We selected a subset of the Pantheon+ light curves with $0.02 < z_{\text{CMB}} < 0.25$ to use as the “Hubble Flow” sample. At redshifts less than 0.02, the distance uncertainties are dominated by galaxy peculiar velocities. The high redshift cut was chosen to avoid a mismatch between the Hubble flow sample and the supernovae typically found in SBF hosts. As we shall see, SNIa in SBF hosts tend to be less luminous than those in actively star-forming galaxies so less likely to be identified in high redshift searches.

2.3. Light Curves for SNe Ia in SBF Hosts

Table 2 lists 33 SNe Ia events that were observed in galaxies with IR SBF distances measured by [Jensen et al. \(2021\)](#) or given in Table 1.

SNe Ia occurring in elliptical galaxies tend to have fast declining light curves and there is overlap between the normal SNe Ia and SN 91bg-like events. SN 91bg-like events are considered peculiar due to their intrinsically red color at maximum light and strong Ti II absorption in their spectra (e.g. [Garnavich et al. 2004](#)). Our SBF sample excludes SNe Ia that were classified as SN 91bg-like from their spectra. The SNANA simulations further removed supernovae that exceed color, stretch, or bias limits (column labeled “SALT2 Fit”). There was no published light curve data available for SN 2017hle. Our sample contains 27 SNe Ia with reliable light curves fits after making these cuts.

For several supernovae there are light curves derived from multiple sources. The Pantheon+ sample calculates separate SALT2 fits for each light curve source. When a supernova had multiple fits, we averaged the distance and SALT2 parameters weighted by their uncertainties. Here, the average difference in SALT2 distance moduli between light curves obtained for the same supernova is 0.027 mag.

Table 2. Type Ia Supernovae in SBF Galaxies

SN	Host	z (CMB)	Stellar Mass (log M_{\odot})	Light Curve Source ^b	SALT2 Fit ^c	Notes
1980N	NGC1316	0.00457(03)	11.77(04)	JRK	yes	Fornax
1981D	NGC1316	0.00457(03)	11.77(04)	JRK	large error	Fornax
1992A	NGC1380	0.00587(15)	11.22(05)	JRK	yes	Fornax
1995D	NGC2962	0.00768(02)	10.84(05)	CFA1	yes	
1997E	NGC2258	0.01314(12)	11.59(06)	CFA2	yes	
1999ej	NGC0495	0.01534(03)	10.93(05)	KAIT, CFA2	yes	
2000cx	NGC0524	0.00697(07)	11.36(05)	KAIT, CFA2	color limit	also 2008Q host
2002cs	NGC6702	0.01532(01)	11.26(05)	KAIT	yes	
2002ha	NGC6964	0.01221(10)	10.96(06)	KAIT, CFA3	yes	
2003hv	NGC1201	0.00511(01)	10.75(05)	KAIT	yes	
2006dd	NGC1316	0.00457(03)	11.77(04)	JRK	yes	Fornax
2006ef	NGC0809	0.01694(01)	10.79(07)	CSP, CFA3	yes	
2006mr	NGC1316	0.00551(04)	11.77(04)	CSP	color limit	91bg-like; Fornax
2007cv	IC2597	0.01362(15)	11.40(05)	SWIFT	yes	
2007gi	NGC4036	0.00505(01)	9.68(06)	JRK	yes	
2007on	NGC1404	0.00594(15)	11.19(05)	CSP, SWIFT	yes	also 2011iv host; Fornax
2008L	NGC1259	0.01733(05)	10.85(07)	CFA3	yes	
2008Q	NGC0524	0.00698(02)	11.36(05)	SWIFT, CFA4	yes	also 2000cx host
2008R	NGC1200	0.01259(15)	11.37(05)	CSP	yes	
2008hs	NGC0910	0.01665(07)	11.45(06)	SWIFT, CFA4	yes	
2008hv	NGC2765	0.01360(07)	11.12(05)	CSP, SWIFT, CFA4	yes	
2008ia	ESO125-G006	0.02257(10)	11.37(10)	CSP	yes	
2010Y	NGC3392	0.01142(01)	10.50(06)	CFA4	yes	
2011iv	NGC1404	0.00519(01)	11.19(05)	CSP	yes	also 2007on host; Fornax
iPTF13ebh	NGC0890	0.01238(05)	11.36(05)	CSP, SWIFT	yes	
2014bv	NGC4386	0.00578(14)	10.86(05)	SWIFT	yes	
2015ar ^a	NGC0383	0.01600(04)	11.45(05)	FOUND	yes	also 2017hle host
2015bo ^a	NGC5490	0.01697(10)	11.48(05)	CSP	stretch limit	91bg-like
2015bp	NGC5839	0.00604(02)	10.53(05)	SWIFT	yes	
2016ajf	NGC1278	0.01977(05)	11.37(07)	FOUND	yes	
2016arc ^a	NGC1272	0.01218(05)	11.60(06)	FOUND	bias correction	
2017hle ^a	NGC0383	0.01600(08)	11.45(05)	none	...	also 2015ar host
2019ein ^a	NGC5353	0.00837(01)	11.37(05)	LOWZ	yes	

^aSN2015ar=PSNJ0107203; SN2015bo=SNhunt278; SN2016arc=ASASSN-16ci; SN2017hle=PSP17E; SN2019ein=ATLAS19ieo

^bReferences – CSP: Burns et al. (2018); JRK: Jha et al. (2007); KAIT: Ganeshalingam et al. (2010); SWIFT: Brown et al. (2018); CFA1: Riess et al. (1999); CFA2: Jha et al. (2006); CFA3: Hicken et al. (2009); CFA4: Hicken et al. (2012); FOUND: Foley et al. (2018) ; LOWZ: Kawabata et al. (2020)

^cDenotes the success of the SALT2 light curve fit or the reason that the fitter failed.

“Sibling” supernovae are multiple events that occurred in the same host galaxy (Scolnic et al. 2020). In our sample, there were several IR SBF galaxies that hosted two or more supernovae. However, after light curve bias cuts, only NGC 1404 (SN 2007on and SN 2011iv) and NGC 1316 (SN 1980N and SN 2006dd) had surviving siblings. Given the small number of siblings, we treat them as independent calibrators.

2.4. Light Curves for SNe Ia in Cepheid Hosts

To compare the IR-SBF distances and their associated supernovae with a set of Cepheid-calibrated hosts and their supernovae, we use the “SH0ES” Riess et al. (2016) sample of SNe Ia. This set of 19 hosts with Cepheid calibrated distances have been recently updated in the Riess et al. (2022) compilation. As a test of consistency, these Cepheids are used to calibrate the same set of Hubble flow supernovae as is done with the IR SBF distances.

3. ANALYSIS

3.1. Direct Comparison of SALT2 and SBF SNe Ia Distances

We compare the SBF distances (Jensen et al. 2021) with the SALT2 SNe Ia distances in Figure 1 (top), where SNe Ia distance modulus uncertainties are taken from the Pantheon+ fits. Because we are directly comparing distance moduli without use of redshifts, we do not add uncertainties due to peculiar velocities. The differences between distance moduli are also shown in Figure 1 (bottom), where their uncertainties have been combined in quadrature.

Assuming the SNe Ia distances and the IR SBF distances differ by a constant, a χ^2 minimization provides an offset of $\Delta M = 0.156 \pm 0.027$ mag in distance modulus. The χ^2 value for the single parameter offset model is 32.4 for 26 degrees of freedom, indicating that the scatter is in fair agreement with the combined uncertainties.

Looking at Figure 1 it is clear that a significant amount of scatter comes from a single Fornax cluster galaxy, NGC 1404, that hosted two SNe Ia (Ashall et al. 2018; Gall et al. 2018). Because SN 2007on and SN 2011iv are essentially at the same distance, we can directly compare the difference in their SALT2 distance moduli and their uncertainties. Their distances differ by nearly 0.5 mag (3.5σ), which should occur at random for only 1 in 2000 siblings (Scolnic et al. 2020). Recalculating the scatter without including the two events in NGC 1404, gives $\chi^2 = 25.2$ for 24 degrees of freedom, suggesting that the combined IR SBF and SNe Ia error estimates for the remaining sample are consistent with the observed scatter. As we have no objective reason to

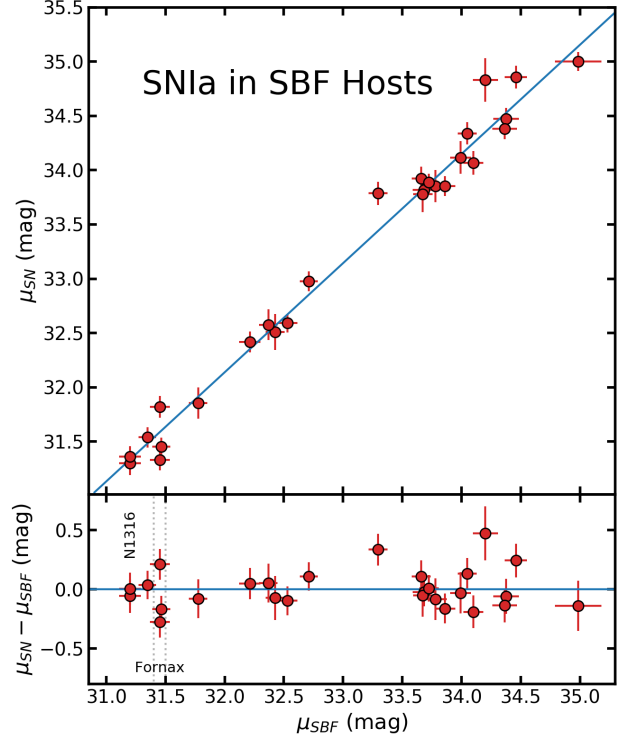


Figure 1. top: The Pantheon+ light curve distances versus the host galaxy IR SBF distances. Distances for SNe Ia with multiple sources of photometric data have been averaged. **bottom:** The difference between the SNe Ia and SBF distance moduli as a function of the SBF distance. The average difference in distance moduli has been subtracted.

exclude NGC1404 or its supernovae, they will remain in the sample for the rest of the analysis.

NGC 1316 is another Fornax cluster galaxy with issues and a detailed review is given by Cantiello et al. (2013). It has hosted multiple SNe Ia and two (SN 1980N and SN 2006dd) made it through all the light curve cuts. However, its IR SBF distance (Table 1) is 0.38 mag (3.4σ) shorter than the Blakeslee et al. (2009) SBF distance. The new IR SBF distance (Table 1) places it in the foreground of the Fornax cluster. NGC 1316 is a giant elliptical galaxy, but with a dusty core that may impact the SBF estimates as well as the SNe Ia distances. SN 1980N occurred far from the galaxy center, but SN 2006dd was projected on a dusty region near the core. Surprisingly, the galaxy does not stand out in Figure 1 because both SNe Ia distances are in good agreement with its IR SBF distance.

As the IR SBF distances to sibling supernovae are not independent in our calculation, we can also average their SALT2 distances and errors to recalculate the χ^2 parameter. After averaging the SNe Ia distances to NGC 1404

and NGC 1316 we see that $\chi^2 = 25.2$ for 24 degrees of freedom.

An important point is that the SNe Ia distance uncertainties are empirically well determined from the large set of Hubble flow events where the scatter added by peculiar velocities is small. That the reduced $\chi^2_{\nu} \approx 1$ for our analysis demonstrates that the uncertainties given in Jensen et al. (2021) accurately describe the scatter in applying the IR SBF method. That the IR SBF uncertainties are typically 0.09 mag implies that the precision of the IR SBF calibration to an individual galaxy is comparable to that of Cepheid calibrators.

3.2. Comparison with Khetan et al.

Khetan et al. (2021) used SBF distances from a wide variety of heterogeneous sources to make an estimate of H_0 . Here, we use the IR SBF distances from Jensen et al. (2021) that have been uniformly analyzed. Only seven of our SBF hosts are included in the Khetan et al. (2021) sample and for these galaxies, the average difference in distance modulus is 0.17 ± 0.11 mag.

The difference between the heterogeneous SBF distances taken from the literature and the consistent sample analyzed here can be seen in the intrinsic scatter of the calibrators. Khetan et al. (2021, Table 4) shows an additional scatter in the calibrator brightnesses of 0.29 mag. In contrast, the scatter we measure using IR SBF distances from Jensen et al. (2021) is consistent with an uncertainty of 0.09 mag in distance modulus.

3.3. Comparison of SNe Ia in SBF- vs. Cepheid-Calibrated Hosts

3.3.1. Light Curve Stretch

The IR SBF method is best applied to massive elliptical galaxies (Blakeslee et al. 2021) with old stellar populations. SBF-calibrated SNIa hosts provide a stark contrast to the Cepheid-calibrated hosts. Cepheid variables are exclusively found in late-type galaxies with young stellar populations. Recent star formation is a prerequisite for containing massive stars that are caught evolving through the instability strip. In addition, SNe Ia in passive galaxies tend to have faster-declining light curves (low stretch values) than SNe Ia in star-forming hosts (Hamuy et al. 1996; Gallagher et al. 2005; Sullivan et al. 2006). Figure 2 compares the SALT2 parameters between the Hubble flow SNe Ia, the SBF-calibrated sample, and the Cepheid-calibrated sample. The SALT2 stretch parameter in the SBF-calibrated sample are seen to be significantly smaller than in the Cepheid-calibrated sample. The transition in light curve widths for SNe Ia in the SBF-calibrated hosts and Cepheid-calibrated hosts is extremely sharp. The cu-

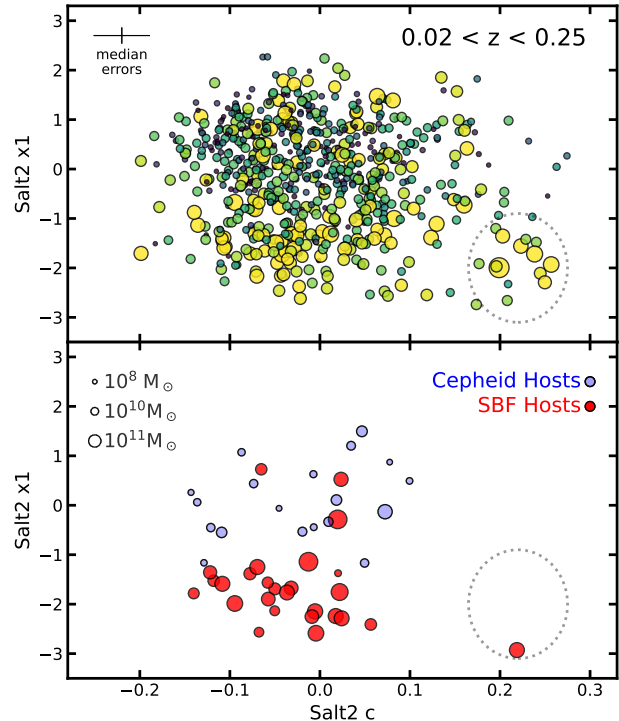


Figure 2. top: The Hubble flow sample showing the SALT2 stretch parameter, x_1 , versus the SALT2 color parameter, c . The point size and color indicate the relative stellar mass of the host galaxy (yellow for more massive hosts). While a wide range of host masses are seen for events with $x_1 > -1$, fast-declining SNe Ia with $x_1 < -1$ tend to occur in very massive hosts. A group of fast declining, red ($c \gtrsim 0.2$) supernovae appear in the lower-right corner of the plot as indicated by the dotted circle. **bottom:** Same as the top plot, but showing the SBF-calibration sample (red) and Cepheid-calibration sample (blue). The SALT2 color distributions are similar between all three samples, but the SBF-calibrated SNe Ia tend to exhibit fast declining light curves ($x_1 < -1.0$) while Cepheid-calibrated SNe Ia exhibit slower decline rates ($-1 \lesssim x_1 \lesssim 2$). One SBF supernova, SN2016ajf, lands in the lower-right of the plot and appears to be a member of the grouping of points noted in the Hubble flow sample.

mulative distributions for the two samples (Figure 3) shows that 89% of the SNe Ia in SBF-calibrated hosts have $x_1 < -1$ while the same fraction of the SNe Ia in Cepheid-calibrated hosts have $x_1 > -1.0$. Therefore, the stretch parameter of $x_1 = -1$ is a natural place to divide the Hubble flow sample when calibrating distances between the two methods.

3.3.2. Color at Peak

Figure 2 shows that the distribution of the SALT2 color parameter, c , is similar between the Cepheid-calibrated sample and the SBF-calibrated sample.

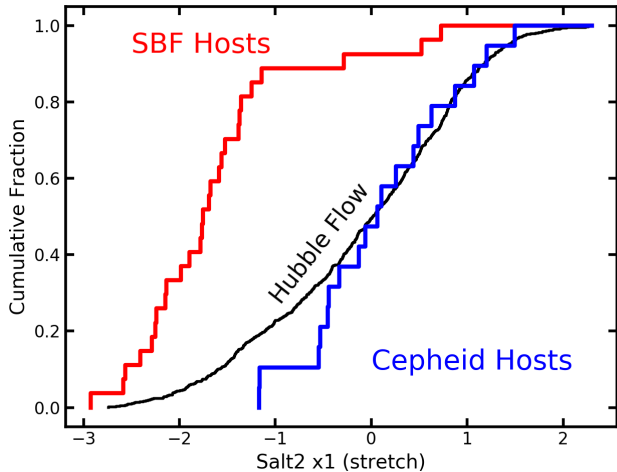


Figure 3. The cumulative distribution of the SALT2 light curve width parameter x_1 for the SBF-calibration sample (red), the Cepheid-calibration sample (blue), and the Hubble flow sample (black). 89% of the SBF-calibrated SNe Ia have $x_1 < -1.0$ and 89% of the Cepheid-calibrated SNe Ia have $x_1 > -1.0$. A minority (22%) of the Hubble flow SNe Ia are fast-decliners with $x_1 < -1.0$.

Based on spectroscopic classifications, we have avoided using SN1991bg-like SNe Ia in the SBF sample. Their colors tend to be redder than normal SNe Ia at maximum and their use as standardizable candles is problematic (Garnavich et al. 2004). We note that in the Hubble Flow sample, there are a number of fast decliners ($x_1 \approx -2$) with reddish peak colors ($c \approx 0.2$) that form a distinct grouping in the lower-right of the Hubble flow sample shown in Figure 2. These passed the color and bias cuts from the SNANA simulations, but are significantly more red than a majority of the SBF-calibrated SNe Ia. One supernova in the SBF-calibration sample (SN2016ajf) shares the peak color and stretch of the group. This small subset of events may represent a transition between normal SNe Ia and the peculiar SN1991bg-like class. Further analysis of these “narrow-normal” SNe Ia is addressed in Milne et al. (in prep).

3.3.3. Host Masses

The stellar masses of the SBF-calibrated host galaxies were estimated using the prescription in Ma et al. (2014). The 2MASS $K_{m,ext}$ magnitude is converted to an absolute magnitude using the distances from Jensen et al. (2021) after correcting for K -band Milky Way dust extinction. The stellar mass estimates are given in Table 2. For the Cepheid-calibrated hosts and the Hubble flow hosts, we take the logarithm of the stellar mass from the Pantheon+ release (Brout et al. 2022).

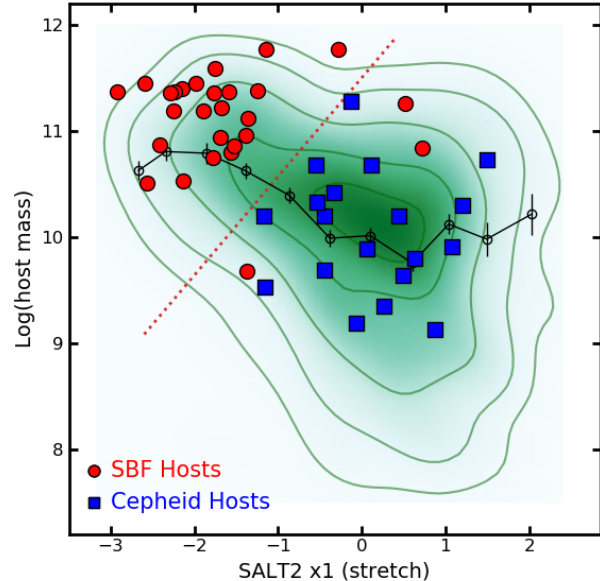


Figure 4. Host stellar mass versus the SALT2 stretch parameter for SBF-calibrated SNe Ia (red) and Cepheid-calibrated SNe Ia (blue). The Hubble flow sample is shown as density contours and as color intensities using a Gaussian density estimator. The open circles show the median log host stellar mass binned in x_1 . For $x_1 < -1$, the median host mass is $10^{10.8} M_{\odot}$, while for $x_1 > -1$ the median host mass remains close to $10^{10.0} M_{\odot}$. For further analysis, we adopt the stretch/mass division between “SBF-like” SNe Ia and “Cepheid-like” SNe Ia shown as the diagonal dotted line (see Section 3.4).

The distribution of host masses shown in Figure 2 suggests that the SBF-calibration sample has significantly more massive hosts than seen in the Cepheid-calibration sample. There are several factors that may contribute to this. For example, SBF is typically applied to bright (thus massive) elliptical galaxies whether or not they have hosted SNe Ia. Thus, a few SNe Ia in our sample exploded in ellipticals with pre-existing SBF measurements. SN2019ein is an example as its host, NGC 5353, was observed as part of the MASSIVE survey (Ma et al. 2014).

Another factor favoring massive hosts in the SBF-calibration sample is that the rate of SNe Ia explosions in passive galaxies appears to be proportional to the host stellar mass, while in star-forming hosts the SNe Ia rate is dominated by the current star formation rate (Scannapieco & Bildsten 2005; Sullivan et al. 2006). So, for elliptical galaxies with no (or very little) star formation, SNe Ia are most likely to appear in hosts with high stellar masses.

The distinction between SNe Ia in SBF-calibrated hosts and Cepheid-calibrated hosts is well shown in

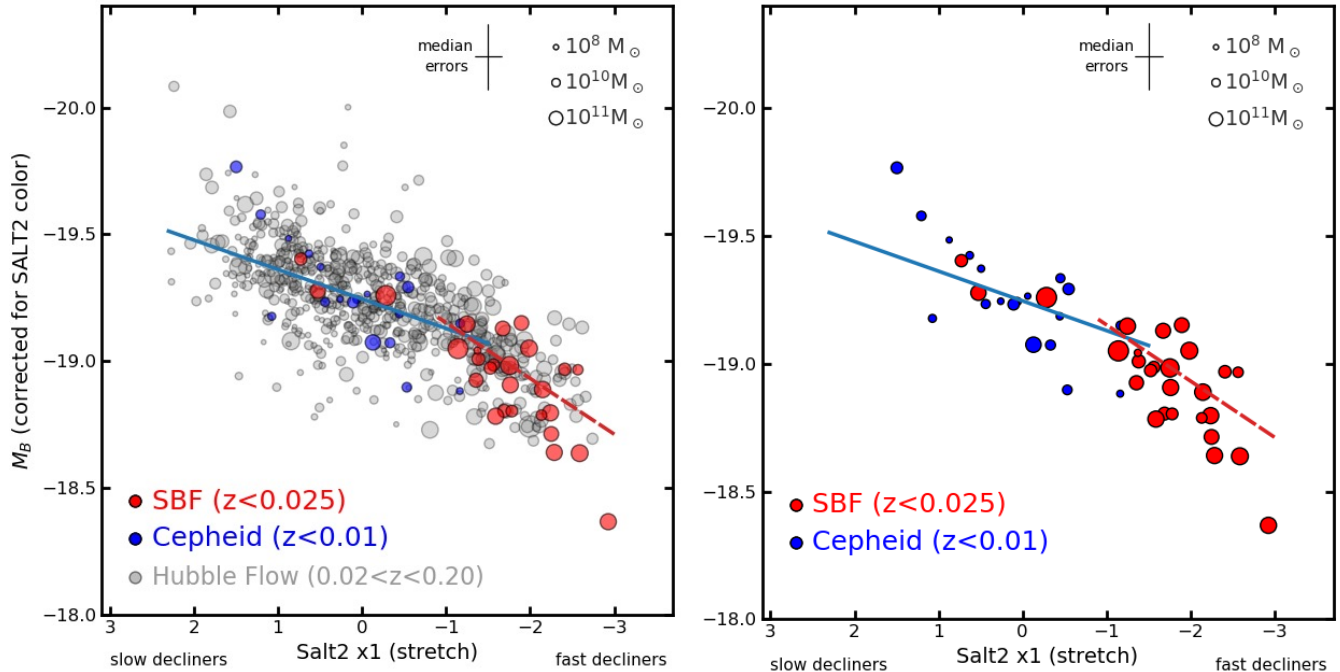


Figure 5. The SNe Ia peak luminosity versus SALT2 stretch parameter (a.k.a. the Phillips diagram) showing the SNe Ia in SBF calibrators (red), Cepheid calibrators (blue) and, in the Hubble flow (grey). For clarity, the right panel is a copy of the left panel without the Hubble flow supernovae plotted. For the Hubble flow sample (grey points), the SNe Ia peak luminosities have been corrected for SALT2 color and distances calculated from the CMB frame redshifts with an assumed $H_0 = 73 \text{ km s}^{-1} \text{ Mpc}^{-1}$. No Pantheon+ bias corrections have been included in the plotted absolute magnitudes. SBF distances and Cepheid distances are used to calculate luminosities of the SBF-calibrated (red) and Cepheid-calibrated (blue) SNe Ia respectively. The SNe Ia host-galaxy mass is indicated by the size of the point. The best fit relation between M_B and $x1$ for events with $x1 > -1.0$ is shown as the solid blue line. The dashed red line is the same but for $x1 < -1.0$. The difference suggests that luminosity correction for SALT2 stretch is non-linear.

Figure 4, where the SALT2 stretch parameter is plotted against host stellar mass. For fast-fading SNe Ia ($x1 < -1$) in the Hubble flow, the median host mass is $10^{10.8 \pm 0.10} M_\odot$, while the median mass drops by nearly an order of magnitude to $10^{9.93 \pm 0.08} M_\odot$ for galaxies hosting slowly fading supernovae. The vast majority of SBF-calibrated host galaxies are significantly more massive than Cepheid-calibrated host galaxies.

A relation between residuals on the Hubble diagram and the stellar mass of SNe Ia host galaxies was noted by Kelly et al. (2010) and confirmed by Sullivan et al. (2010) and Lampeitl et al. (2010). An empirical correction has commonly been applied as a “mass step” (e.g. Betoule et al. 2014; Kelsey et al. 2021) occurring at $M_\star = 10^{10} M_\odot$, although the physical origin of the correlation remains uncertain. Parameters such as host mass, metallicity, stellar age, star-formation rate, and light curve width show correlations that may be related to trends in galactic evolution and the SNe Ia delay-time distribution (Rose et al. 2019; Childress et al. 2014). Recently, Brout & Scolnic (2021) argued that the apparent

mass step is a result of differing dust properties between massive and low-mass hosts and it is not intrinsic to SNe Ia luminosities. The bias corrections applied to the Pantheon+ light curves mitigates the mass-step issue in the resulting SNe Ia distance estimates.

3.3.4. Phillips Relation

The relation between light curve decline rate and peak luminosity for SNe Ia is often referred to as the Phillips relation (Phillips 1993). We plot the Phillips relation for the Hubble flow, the SBF-calibrated, and Cepheid-calibrated samples in Figure 5. The SALT2 stretch parameter, $x1$, is used as the light curve decline rate indicator. The luminosity is estimated from the apparent peak magnitude, m_B , corrected for the SALT2 color term using $\beta = 3.09$. No correction for stretch has been applied in Figure 5. For the Cepheid and SBF-calibrated SNe Ia, we adopted distances from Riess et al. (2022) and Jensen et al. (2021). For the purposes of plotting the absolute magnitudes that are consistent with the calibrators, we calculated the distance moduli

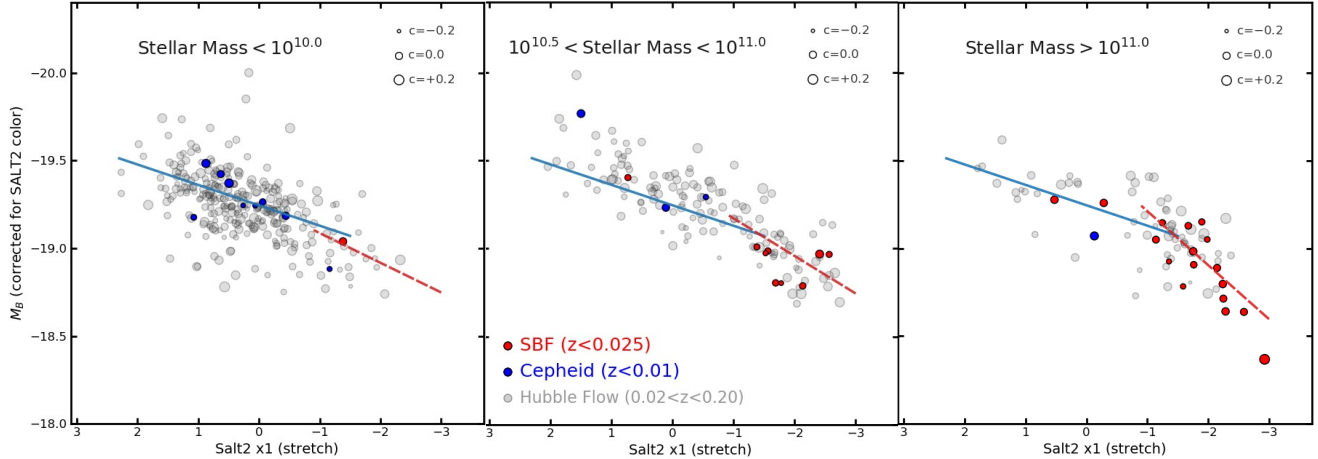


Figure 6. The Phillips relation divided into host stellar mass bins. In this figure, the sizes of the circles represent the SALT2 color of the SN Ia at peak. No Pantheon+ bias corrections have been included in the plotted absolute magnitudes. The solid blue line in all the panels shows the best fit to all SNe Ia with $x1 > -1$ as calculated for Figure 5. The blue points show the SNe Ia in Cepheid-calibrated hosts and the red points are SNe Ia in SBF-calibrated hosts. **left:** The Phillips relation for SNe Ia in low-mass hosts. The red dashed line is a fit to the points with $x1 < -1$ and the slope is similar to that of the slow decliners. **center:** The Phillips relation again, but for intermediate mass hosts. Note that SNe Ia with $x1 > -1$ generally sit above the blue line indicating the “mass-step” has been crossed. The shift in luminosity between the left and center panels for $x1 > -1$ is 0.10 mag. For SNe Ia with $x1 < -1$, the slope has steepened slightly from the left panel at 0.16 to 0.21 for the intermediate masses. **right:** The Phillips relation for very high mass hosts. Note that there are very few slow decliners for this mass range. For $x1 < -1$, the best fit slope further steepens to $\alpha = 0.31$.

for the Hubble flow sample from their redshift in the CMB frame and corrected for cosmological parameters assuming $H_0 = 73 \text{ km s}^{-1} \text{ Mpc}^{-1}$. Here, the choice of H_0 is arbitrary and this value was chosen to approximate the expected supernova absolute magnitudes. Selecting $H_0 = 68 \text{ km s}^{-1} \text{ Mpc}^{-1}$ would shift all the points by 0.15 mag along the y-axis. No Pantheon+ bias corrections have been applied to the supernovae shown in Figure 5.

A weighted linear regression for all SNe Ia with $x1 > -1$ gives a slope of $\alpha_{slow} = 0.11 \pm 0.02$ while the slope for the fast decliners with $x1 < -1$ is $\alpha_{fast} = 0.212 \pm 0.023$. Removing the extremely fast and red SN2016ajf from the fit, changes the estimated slope to -0.207 ± 0.023 (a shift of 0.2σ). The α calculated from the entire Pantheon+ bias-corrected set (Brout et al. 2022) gives a slope of $\alpha = 0.148 \pm 0.003$, which lies between the slopes found for the sets divided by stretch.

Without the bias-correction, the stretch/luminosity correction in the Tripp relation (Equation 1) should include a non-linear term to account for the sharp change in slope between fast and slow fading SNe Ia. The Phillips relation using the $\Delta m_{15}(B)$ was improved by applying a quadratic function (Phillips et al. 1999). Recently, Burns et al. (2018) applied a color-stretch parameter that shows a clear non-linear relationship between light curve decline rate and luminosity ranging from ultraviolet to the near-infrared bands. Ashall et al. (2020)

found a change in the color-stretch parameter luminosity relation near $s_{BV} = 0.71$ which corresponds to a SALT2 stretch of $x1 \approx -1.5$. This transition corresponds to an absolute magnitude of $M_B = -19.0$

Because the SBF- and Cepheid-calibration samples radically differ in host stellar mass, we show the Phillips relation for three mass cuts in Figure 6. We again see that the Cepheid-calibrated galaxies dominate the low-mass bin while the SBF-calibrated galaxies are found mainly in the intermediate-mass and high-mass subsamples. Again, the Pantheon+ bias corrections have not been applied for these plots.

For the slow declining SNe Ia ($x1 > -1.0$), there is very little change in the luminosity slope for the different mass cuts, but the mass-step is clearly seen going from the low-mass to intermediate-mass samples. That is, the SNe Ia in intermediate-mass hosts tend to be nearly 0.1 mag brighter than SNe Ia in low-mass hosts. Given the relatively few slow-decliners in the very highest mass bin, it is difficult to define a trend there.

For fast-decliners ($x1 < -1.0$), the error-weighted linear regression used to estimate the slope in Figure 6 steepens with increasing host mass. For the highest host-mass bin, the luminosity slope is twice the value measured for the full sample, that is, -0.308 ± 0.043 versus -0.135 ± 0.005 (a difference of 4.0σ). When SN2016ajf is excluded from the fit, the slope of the high-

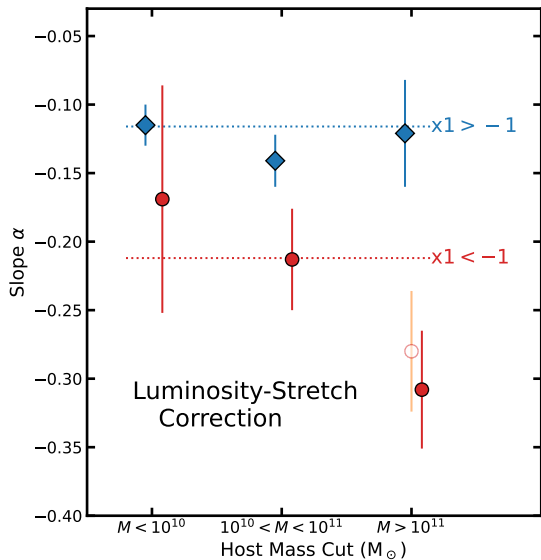


Figure 7. The slope, α , of the correlation between luminosity and light curve stretch for various subsets of SNe Ia discussed in Section 3. The SNe Ia were divided into slow decliners with stretch parameters of $x1 > -1$ (shown as blue diamonds), and fast decliners with stretch parameters of $x1 < -1$ (shown as red circles). The dotted lines show the slope estimated using the full range of host galaxy masses. The points indicate the slopes measured using SNe Ia divided into three host mass bins. The open circle shows the measured slope when the extreme SN2016ajf is excluded from the fit in the highest host mass bin.

est host-mass sample becomes -0.280 ± 0.045 (a shift of 0.7σ).

In Figure 7, we summarize the estimated slopes (and uncertainties) for the fast and slow decliners over three host mass ranges. For light curves with $x1 > -1$, the estimated slopes are consistent over all three host mass bins. For fast declining SNe Ia ($x1 < -1$), there is an indication that α gets steeper with increasing host mass.

Figures 5 and 6 suggest that it is risky to apply a simple Tripp relation to SNe Ia found in massive, early-type hosts such as those used in measuring SBF distances. The bias corrections calculated for the Pantheon+ distances (Brout et al. 2022) attempt to mitigate the observed non-linear variations over stretch. A complementary approach used here is to isolate Hubble flow supernovae that share characteristics of SNe Ia in SBF-calibrators and to refit the linear Tripp parameters.

3.4. The Hubble Constant

The previous sections show that SNe Ia events in Cepheid-calibrated hosts and SBF-calibrated hosts are

very different in their properties. While their colors near maximum have similar distributions (see Figure 2), SNe Ia in Cepheid-calibrated hosts tend to be slow decliners in low-mass hosts while SNe Ia in SBF-calibrated hosts tend to be fast decliners in high-mass hosts. To understand the impact on H_0 that may result from calibrating Hubble flow with supernovae and hosts that possess strongly divergent properties, we will first estimate H_0 based on the full Hubble flow sample and then by dividing the Hubble flow sample into subsets that match the properties of the calibrators.

The “full” Hubble flow sample consists of 816 SNe Ia with $0.02 < z_{\text{CMB}} < 0.25$. The full sample is divided into “fast” and “slow” sub-samples at $x1 = -1.0$. To test for systematics, the fast sub-sample is calibrated with the Jensen et al. (2021) SBF distances and the slow sub-sample is calibrated using the Cepheid distances from SH0ES (Riess et al. 2016, 2022). The SNe Ia distances in the “full”, “fast”, and “slow” sub-samples are taken from the bias-corrected Pantheon+ sample (Brout et al. 2022)

The SBF calibration sample consists of supernovae and their host galaxies that are distinct from the typical SNe Ia in the Pantheon+ sample. The SBF-calibration sample is dominated by fast-declining supernovae that have exploded in massive, passive galaxies. To select a Hubble flow sample as close as possible to the characteristics of events in the SBF-calibration sample, we must use both the light curve stretch parameter and the host mass to define a “SBF-like” sample. This is an odd name, but it concisely captures the goal of matching the characteristics of the SBF-calibrated galaxies and their supernovae. We define the SBF-like sub-sample in both stretch and host mass using the relation,

$$\log_{10}(\text{mass}) = 0.93(x1) + 11.5, \quad (2)$$

as shown by the red dotted line in Figure 4. Events above this relation are designated “SBF-like.” The SBF-like sample consists of 162 Hubble flow supernova and 24 SBF-calibrators. For this sub-sample we do not use the Pantheon+ bias corrections. Instead, selecting only the SBF-like events, we refit the SALT2 stretch and color coefficients to minimize scatter in the Hubble flow and apply these revised coefficients to the SNe Ia hosted by SBF-calibrated galaxies.

3.4.1. The Hubble Flow Distances

Riess et al. (2009) outlined the steps needed to calibrate SNe Ia occurring in Cepheid-calibrated host galaxies and apply that to the Hubble flow. Cosmological effects become important in the Hubble flow, so the equation relating the local Hubble parameter with redshift includes deceleration/acceleration correction terms

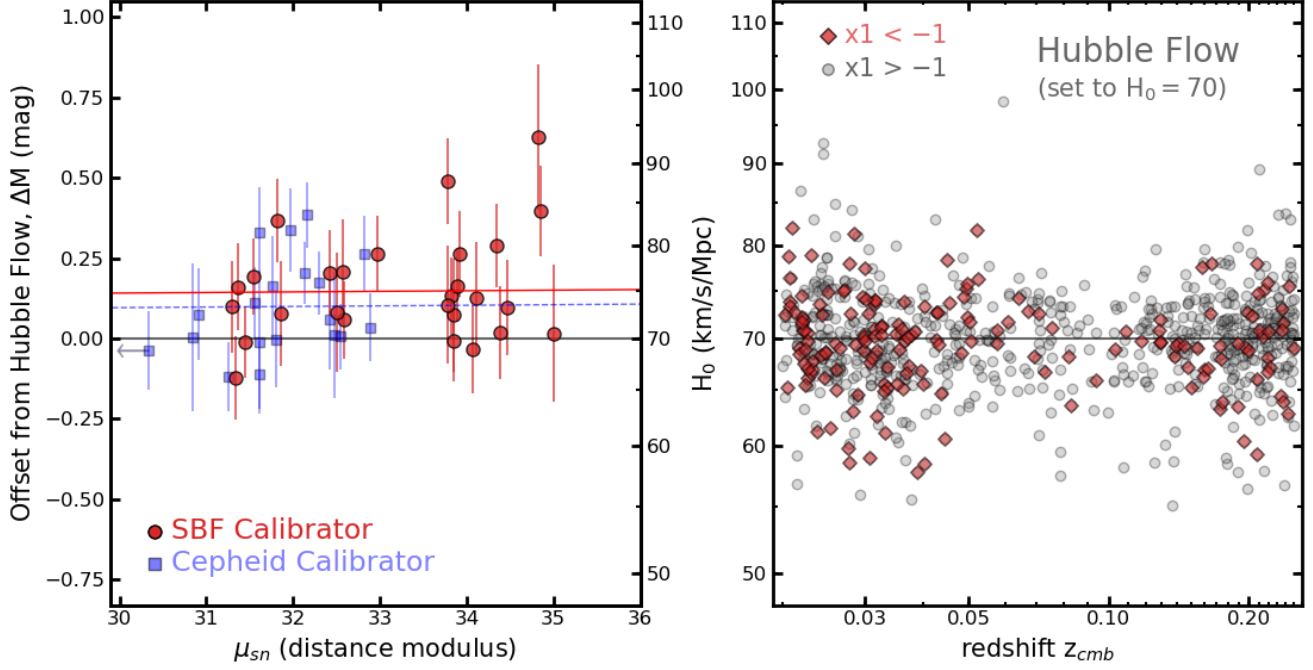


Figure 8. H_0 estimated from SBF and Cepheid calibrators using the Pantheon+ light curves anchored by the Hubble flow. **left panel:** Each SBF-calibrated event (red points) provides an estimate of H_0 based on the offset between the SBF distance and the SALT2 distance. The blue points are the same but for the Cepheid-calibrated SNe Ia from Riess et al. (2016). Both the SBF- and Cepheid-calibrated events suggest a value for H_0 greater than $70 \text{ km s}^{-1} \text{ Mpc}^{-1}$. The average of the H_0 estimates from SBF-calibrated SNe Ia is shown as the red solid line. SN 2011fe has been shifted in distance to make the plot more readable. **right panel:** The Hubble flow supernovae for $0.02 < z_{cmb} < 0.25$, displaying the scatter about their mean luminosity. The luminosity has been set to provide an $H_0 = 70 \text{ km s}^{-1} \text{ Mpc}^{-1}$. The light red points indicate supernovae with light curve stretch values of $x1 < -1.0$, similar to the SNe Ia from SBF hosts.

in the form of expansions in redshift. We modify Equation 14 from Riess et al. (2009) to directly use the distance moduli output by SALT2, μ_{s2} . These SALT2 distances have been calculated based on Equation 1 with the fiducial SNe Ia absolute magnitude, M_B , assigned an arbitrary value. Thus, the μ_{s2} values can be shifted by a constant, ΔM , that is equivalent to varying M_B . That is, the SBF (or Cepheid) calibrators are used to estimate ΔM and from it, H_0 . We define a parameter, $\log H_{s2}$, based on the Hubble flow SALT2 distance moduli:

$$\log H_{s2} = \log cz \left\{ 1 + \frac{1}{2}[1 - q_0]z - \frac{1}{6}[1 - q_0 - 3q_0^2 + j_0]z^2 \right\} - 0.2\mu_{s2} + 5, \quad (3)$$

where z is the redshift in the CMB frame, q_0 , is the deceleration parameter, and j_0 is the jerk parameter. We set $q_0 = -0.54 \pm 0.06$ with j_0 fixed at 1.0 (Riess et al. 2022). Each supernova in the Hubble flow provides a $\log H_{s2}$ value, and a weighted average is calculated. The

resulting average $\log H_{s2}$ for each sub-sample is given at the bottom of Table 3.

The difference between each calibrator distance modulus, μ_{calib} , and its corresponding supernova SALT2 distance modulus, μ_{s2} , provides the magnitude offset, $\Delta M = \mu_{s2} - \mu_{calib}$, from the arbitrary M_B assumed during the SALT2 fitting. Working directly with distance moduli, each SNe Ia in a calibrated host provides an estimate of H_0 through,

$$\log H_0^i = \log H_{s2} + 0.2(\mu_{s2}^i - \mu_{calib}^i), \quad (4)$$

where the superscript, i , indicates the individual calibrators. The estimated H_0 and statistical uncertainties from the SBF calibrators, the Cepheid calibrators, and the various sub-samples are given at the top of Table 3.

The parameter $\log H_{s2}$ depends only upon the SALT2 supernova distances in the Hubble flow and its variation between supernova sub-samples provides a test of systematic errors in the Pantheon+ light curve fits and bias corrections. As seen in Table 3, the parameter does not vary significantly for the different SNe Ia Hubble flow subsets. This suggests that any systematic differ-

ences between the fast ($x1 < -1$) and slow ($x1 > -1$) subsets have been mitigated through the bias corrections from the SNANA simulations and applied in the Pantheon+ compilation. Because of the small number of events in the fast sub-sample ($x1 < -1$), the uncertainty on $\log H_{s2}$ is significantly larger than for the other samples.

4. RESULTS

4.1. Full Sample

H_0 estimates from the SBF and Cepheid calibrators are displayed in the left panel of Figure 8. The SBF calibrator distances average 0.15 mag fainter than the SALT2 SNe Ia distance moduli when the M_B parameter is set to yield $70.0 \text{ km s}^{-1} \text{ Mpc}^{-1}$ in the Hubble flow (right panel of Figure 8). More precisely, the SBF-calibrators applied to the full Hubble flow supernova sample provide an estimate of $H_0 = 74.61 \text{ km s}^{-1} \text{ Mpc}^{-1}$ with a statistical uncertainty of $\pm 0.93 \text{ km s}^{-1} \text{ Mpc}^{-1}$ as shown in Table 3. The Cepheid calibrators applied to the Hubble flow supernovae yield $H_0 = 73.07 \pm 0.96 \text{ km s}^{-1} \text{ Mpc}^{-1}$, and this is consistent with the measurement by [Riess et al. \(2022\)](#). We note that Figure 8 shows that the SBF-calibrators extend two magnitudes further in distance modulus than the Cepheid-calibrated SNe Ia, thus, the SBF calibrators reach the near edge of the Hubble flow as defined here.

4.2. Fast vs. Slow Sub-samples

Using only fast-declining SNe Ia results in an insignificant shift in the estimated H_0 value when compared with the Full sample. Table 3 shows that the 175 Hubble flow events with $x1 < -1.0$ and calibrated with IR SBF distances shift the H_0 estimate by less than $0.2 \text{ km s}^{-1} \text{ Mpc}^{-1}$. Calibrating the slow-fading SNe Ia with Cepheid distances also has a minimal impact on the results.

4.3. SBF-like Sub-sample

In the previous analyses, we applied calibrations using supernova distances conditioned using bias corrections derived from SNANA simulations ([Brout et al. 2022](#)). This approach works very well as demonstrated by the consistent results when sub-samples of the Hubble flow supernovae are analyzed. But there remains concern that the unique character of SNe Ia found in SBF-calibrated galaxy (“SBF-like” supernovae defined in Section 3.4) may not be fully accounted for in the simulations. For the 162 Hubble flow SNe Ia in the SBF-like sub-sample, we refit the SALT2 α and β parameters so as to minimize their Hubble residuals. In this sub-sample, the typical stretch parameter value is $x1 < -1$,

so we recenter the stretch distribution using a modified Tripp relation:

$$\mu = m_B + \alpha (x1 + 1.5) - \beta c - M_B, \quad (5)$$

which avoids creating a large correlation between α and M_B . We then estimate H_0 by applying the new SALT2 coefficients to IR SBF-calibrated SNe Ia light curves and averaging the results from Equation 4.

We ran a Markov-Chain Monte Carlo (MCMC) calculation on the SBF-like Hubble flow supernovae to determine the SALT2 parameters that minimize the Hubble residuals. The MCMC code then applies these parameters to the 24 SNe Ia in the SBF calibration sample that meet the stretch and host mass criteria. The SALT2 parameters and the resulting H_0 are shown in Figure 9. As expected, the luminosity slope ($\alpha = 0.23 \pm 0.02$) is found to be very steep when compared with the slope for the slow-decliners. The color correction parameter ($\beta = 2.7 \pm 0.1$) is similar to that found for the Full sample.

The fiducial absolute magnitude after refitting, $M_B = -19.14$, is fainter than that shown in Figure 5 because here we reference to a stretch parameter of $x1 = -1.5$ instead of $x1 = 0.0$. Applying these parameters to the Hubble flow supernovae and the SNe Ia in the SBF calibrators results in an H_0 value that is $1.5 \text{ km s}^{-1} \text{ Mpc}^{-1}$ smaller than the results from the Pantheon+ distances, but within the statistical uncertainties of the two methods. The $H_0 = 73.31 \pm 0.99(\text{stat})$ estimated from the SBF-like sample with refitted SALT2 coefficients is nearly identical to that found by [Blakeslee et al. \(2021\)](#) using IR SBF measurements as their “top rung.” Both are in excellent agreement with the [Riess et al. \(2022\)](#) Cepheid measurement of H_0 (see Figure 10).

4.4. The Hubble Constant

As shown in the previous sections, the IR SBF distance measured to SNe Ia hosts allows us to calibrate the Hubble flow supernovae and estimate the Hubble constant with a zero point established from Cepheid variables. Using the full Hubble flow sample of Pantheon+ supernova distances results in $H_0 = 74.61 \text{ km s}^{-1} \text{ Mpc}^{-1}$ with a statistical uncertainty of $0.93 \text{ km s}^{-1} \text{ Mpc}^{-1}$.

Dividing the SNe Ia into subsamples based on light curve and host properties moves the calibration at the 0.03 mag level. Thus, we include a systematic uncertainty of 1.8% on the H_0 estimate caused by the differences between SNe Ia found in SBF-calibrated hosts and supernovae exploding in star-forming host galaxies. In addition, the zero point of the IR SBF distances has a systematic uncertainty of 3.1% based on the [Blakeslee](#)

Table 3. H_0 from SNe Ia Samples

Calibration	Hubble Flow ^a	Number of	Reduced	σ	$\overline{\mu_{s2} - \mu_{calib}}$	H_0^b
Sample	Sample	SNe Ia	χ_ν^2	(mag)	(mag)	(km s ⁻¹ Mpc ⁻¹)
SBF (Full)	Full	27	1.25	0.153	0.154±0.027	74.61±0.93
SBF ($x1 < -1$)	Fast	24	1.37	0.160	0.162±0.028	74.80±1.03
Cepheids (Full)	Full	19	1.61	0.153	0.109±0.028	73.07±0.96
Cepheids ($x1 > -1$)	Slow	17	1.75	0.164	0.100±0.031	72.75±1.04

Hubble Flow ^c	Number of	Reduced	σ	$\log H_{s2}^d$
Sample	SNe Ia	χ_ν^2	(mag)	
Full	816	1.12	0.135	1.8420±0.0009
Fast: $x1 < -1.0$	175	1.01	0.144	1.8415±0.0020
Slow: $x1 > -1.0$	641	1.16	0.152	1.8421±0.0010

^aIndicates the Hubble Flow sample used to estimate $\log H_{s2}$

^bUncertainties are statistical only and include the error from the Hubble Flow

^cThe Hubble flow redshift range: $0.02 < z < 0.25$

^dThe $\log H_{s2}$ parameter is defined in Equations 3 and 4.

et al. (2021) SBF calibration. A summary of statistical and systematic errors contributing to our Hubble constant estimate is given in Table 4.

The IR SBF/SNe Ia derived Hubble constant is consistent with the Cepheid/SNe Ia based on the Riess et al. (2022) distances. Because the IR SBF zero point is based on Cepheids (Jensen et al. 2021), we expect that the 2% shift in H_0 (Table 3) may be a result of the extreme differences in SNe Ia properties between star-forming hosts and massive, passive hosts. Indeed, the largest offset ($\sim 3\%$) is seen between IR SBF-calibrated hosts using only fast-fading supernovae, and the Cepheid-calibrated hosts using only slow-fading events.

5. DISCUSSION

SNe Ia in SBF-calibrated hosts appear quite different from those in Cepheid-calibrated hosts. The majority of light curves in the SBF-calibrated sample are narrow ($x1 < -1.0$) and are found in hosts with stellar masses greater than $10^{10.5} M_\odot$. These differences suggest a possible systematic shift between SBF and Cepheid calibrations, but no significant systematic is found based on the consistency in H_0 estimated from various sub-samples of the Pantheon+ SNe Ia.

The SNANA simulations and resulting bias corrections of the SNe Ia light curve parameters appears to

have successfully mitigated significant systematic differences between the SBF- and Cepheid-calibrated SNe Ia populations. Further, our test of isolating SBF-like SNe Ia and refitting SALT2 coefficients also appears to have resulted in a calibration consistent with the calibration of the entire SNe Ia sample. The SBF method as a calibrator of the Hubble flow SNe Ia does not appear biased relative to other methods. However, the IR SBF distance scale is calibrated using a Cepheid zero point, so is not completely independent of other methods, and is subject to the same common systematic uncertainties at lower rungs of the distance ladder.

The physical origin of the extreme differences between SNe Ia occurring in SBF-calibrated hosts and Cepheid-calibrated hosts remains uncertain. The difference in light curve width between elliptical and spiral host galaxies is well known (Hamuy et al. 1996; Gallagher et al. 2005), and maybe more evident here because the SBF method selects the most extreme hosts in age and mass. This is contrasted with the Cepheid-calibrated SNe Ia that tend to originate in hosts that require some recent star formation and are lower in mass than the passive hosts. There is certainly a formation-to-explosion delay-time difference between the SBF-calibrated and Cepheid-calibrated supernovae. It remains unclear if all SNe Ia events arise from a single progenitor whose explosion properties evolve with age or result from multiple

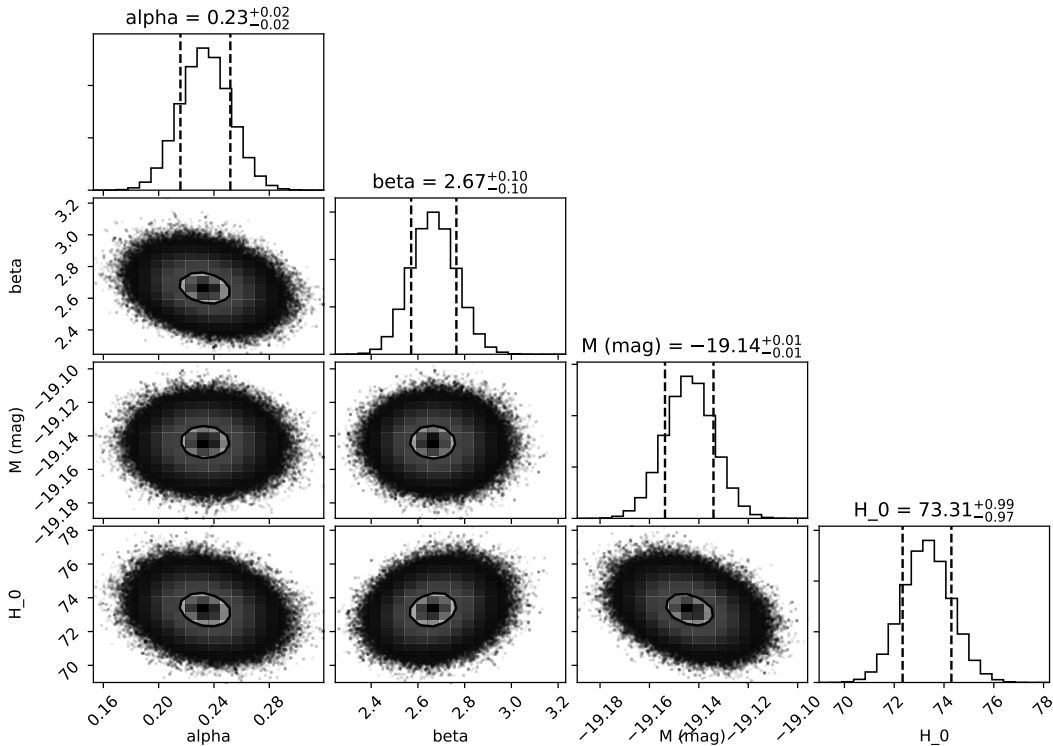


Figure 9. The MCMC results for refitting the SALT2 parameters using Hubble flow SNe Ia with fast-declining light curves in massive hosts (SBF-like events). The revised SALT2 parameters are then applied to the SBF-calibrated SNe Ia and H_0 is estimated from the IR SBF distances. The resulting H_0 estimate is consistent with that from Cepheid-calibrated SNe Ia.

progenitor mechanisms that overlap in their observable properties.

Excluding the fast decliners, Figure 6 clearly shows that the average peak luminosity from the SALT2 analysis of light curves is 0.1 mag brighter for SNe Ia in high-mass hosts, which is the origin of the “mass-step” correction. Brout & Scolnic (2021) have argued that this is due to changes in dust properties with increasing galaxy mass. A recent study by Chen et al. (2022) suggests that the relation between color and luminosity for SNe Ia found in massive passive hosts is flatter than seen in star-forming galaxies.

For the fast-declining SNe Ia shown in Figure 6, there is a clear increase in the α parameter moving from low to high mass hosts. In fact, the absolute peak magnitude of supernovae with stretch $x1 < -1$ are best fit with an extremely steep $\alpha = 0.31 \pm 0.05$. We are likely seeing an increasing fraction of low-luminosity supernovae in the most massive hosts. While we have culled events that are spectroscopically identified as SN1991bg-like, there may be a transition between fast-declining “narrow normals” and true SN1991bg-like events that results in the steepening slope seen in the Phillips relation. This transition could be identified with the SNe Ia in the lower-right of Figure 2 where there is a cluster of reddish/fast-decliners in massive hosts. Our lowest luminosity SNe

Table 4. Uncertainties on H_0 from IR SBF

Source	Type	σ (mag)	H_0
IR SBF/SNe Ia hosts	stat	0.027	1.2%
Hubble flow	stat	0.005	0.2%
SNe Ia samples	syst	0.038	1.8%
Zero point ^a	syst	0.066	3.1%
Total	stat	0.027	1.2%
Total	syst	0.076	3.6%

^aFrom Blakeslee et al. (2021).

Ia in the SBF calibration sample, SN2016ajf, is likely a member of this group. The fact that SN2016ajf passed all the SNANA bias cuts suggests that these transition events may still be useful as distance indicators and calibrators.

6. CONCLUSION

We have used new IR-SBF distances to 25 unique SNe Ia host galaxies to calibrate the luminosity of a large set of Hubble flow SNe Ia. We have tested the robustness of the calibration in three ways. First, we used Pantheon+ bias-corrected distances to estimate the Hubble

constant from SBF and Cepheid calibrators. Second, we divided the Hubble flow sample into sub-samples with properties similar to that of the calibrator samples. Finally, we identified supernovae in the Hubble flow that simultaneously matched the stretch parameters and host galaxy masses of the SBF calibrators. We then refit their light curve correction coefficients to obtain distances that were independent of the Pantheon+ bias corrections. We then searched for systematic shifts in the Hubble constants derived from these techniques. A summary of our results is shown in Figure 10 and described here:

- Directly comparing the SALT2 SNe Ia distances and IR SBF distances demonstrates that the estimated uncertainties given in [Jensen et al. \(2021\)](#) accurately reflect the observed scatter. Distance uncertainties to individual IR SBF hosts are comparable to uncertainties in the Cepheid calibrators.
- The light curve widths for the SBF-calibrated SNe Ia are typically extremely narrow when compared to the Cepheid-calibrated SNe Ia, with 24 of 27 of the SBF-calibrated SNe Ia having a stretch parameter of $x1 < -1.0$ while only 2 in 19 of the Cepheid-calibrated SNe Ia are seen to fade so quickly. The distribution of SNe Ia colors at peak is similar between SBF- and Cepheid-calibrated SNe Ia when SN1991bg-like events are excluded.
- The majority of SBF-calibrator galaxies possess larger stellar masses than the star-forming spirals calibrated by Cepheids. All but one of the SBF-calibrator galaxies has a stellar mass above the typical location of the “mass-step” at $10^{10} M_{\odot}$, while the median galaxy mass of Cepheid-calibrators is just below $10^{10} M_{\odot}$.
- The relation between SNe Ia peak brightness and light curve width appears to steepen with decreasing stretch (SALT2 $x1$), suggesting that the linear Tripp relation should be modified when applied to fast declining events. Other fitters (e.g. [Phillips et al. 1999](#); [Burns et al. 2018](#)) have seen such a non-linear relationship between luminosity and light curve width.
- We find the difference between the IR-SBF calibration and Cepheid calibration of the Hubble flow supernovae to be 0.045 ± 0.038 mag or a $2.0 \pm 1.7\%$ difference in H_0 .
- When the sample was restricted to SNe Ia with narrow light curves ($x1 < -1.0$, the “fast” sub-sample), the estimated Hubble constant changed

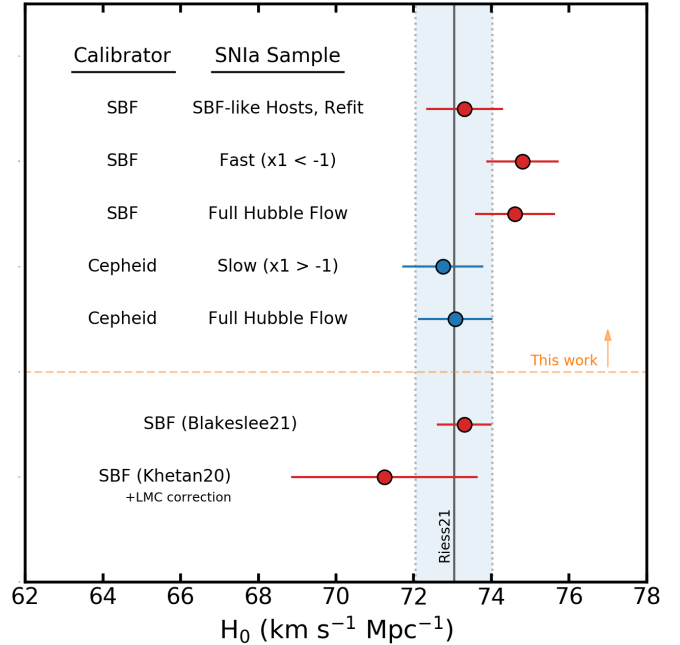


Figure 10. The results of this work compared with Hubble constant estimates using SBF from [Khetan et al. \(2021\)](#) and [Blakeslee et al. \(2021\)](#). Errorbars on points indicate statistical uncertainties only. The light blue band is the [Riess et al. \(2022\)](#) estimate using Cepheids (indicating combined statistical and systematic uncertainties). The top-most point shows the results from fitting supernova luminosity corrections trained on fast-declining SNe Ia occurring in massive host galaxies (SBF-like events). Our other results use the Pantheon+ bias-corrected SALT2 SNe Ia distances.

by only $0.19 \text{ km s}^{-1} \text{ Mpc}^{-1}$ compared with the estimate that used the full range of stretch. Thus, there is no significant shift between the full Hubble flow and the sample containing only fast fading supernovae. We conclude that bias corrections derived from SNANA simulations are effective at reducing systematic distance residuals across the full range of light curve decline rates.

- Refitting SALT2 parameters using only SNe Ia in the “SBF-like” sub-sample (selected by both host mass and stretch parameter), we find a steep luminosity slope $\alpha = 0.23 \pm 0.02$ best corrects the SNe Ia luminosities. The Hubble constant derived from the revised SALT2 parameter fit and calibrated with IR SBF distances is $H_0 = 73.3 \pm 1.0 \text{ km s}^{-1} \text{ Mpc}^{-1}$, or within 0.3% of the H_0 derived from the Cepheid-calibrated SNe Ia sample.
- Using IR SBF distances to calibrate the Pantheon+ SNe Ia and then applying this calibration to Pantheon+ SNe Ia in the Hubble flow, we estimate $H_0 = 74.6 \pm$

$0.9(\text{stat})\pm 2.7(\text{syst}) \text{ km s}^{-1} \text{ Mpc}^{-1}$. The IR SBF zero point is based on Cepheid distances, so this is not a fully independent test of the Hubble tension. But, the consistency between the IR SBF and Cepheid calibrators suggests that the top rung of the SNe Ia distance ladder is not a major source of the Hubble tension.

We find that the IR SBF method for calibrating distances is competitive with the Cepheid calibration of nearby SNe Ia. Despite the divergent properties we identify between SNe Ia found in star-forming and massive/passive hosts, we find no significant systematic difference between the SBF and Cepheid calibrators when using the bias-corrected Pantheon+ distances or refitting the luminosity/stretch relation for fast fading SNe Ia.

Compared to Cepheid calibrations, the IR SBF method can reach more distant SNe Ia hosts with a lower observing time cost per calibrator. The angular resolution of JWST is likely to boost the reach of IR-SBF distance measurements. Nearby, the JWST calibration of distance indicators found in old populations, such as the TRGB, may lead to a robust distance ladder out to the Hubble flow that is independent of Cepheids and further test the origin of the Hubble tension.

ACKNOWLEDGMENTS

We thank Rebecca Chen for comparing these results to the Khetan et al. distances.

REFERENCES

- Ashall, C., Mazzali, P. A., Stritzinger, M. D., et al. 2018, *MNRAS*, 477, 153, doi: [10.1093/mnras/sty632](https://doi.org/10.1093/mnras/sty632)
- Ashall, C., Lu, J., Burns, C., et al. 2020, *ApJL*, 895, L3, doi: [10.3847/2041-8213/ab8e37](https://doi.org/10.3847/2041-8213/ab8e37)
- Bernal, J. L., Verde, L., & Riess, A. G. 2016, *JCAP*, 2016, 019, doi: [10.1088/1475-7516/2016/10/019](https://doi.org/10.1088/1475-7516/2016/10/019)
- Betoule, M., Kessler, R., Guy, J., et al. 2014, *A&A*, 568, A22, doi: [10.1051/0004-6361/201423413](https://doi.org/10.1051/0004-6361/201423413)
- Blakeslee, J. P., Jensen, J. B., Ma, C.-P., Milne, P. A., & Greene, J. E. 2021, *ApJ*, 911, 65, doi: [10.3847/1538-4357/abe86a](https://doi.org/10.3847/1538-4357/abe86a)
- Blakeslee, J. P., Jordán, A., Mei, S., et al. 2009, *ApJ*, 694, 556, doi: [10.1088/0004-637X/694/1/556](https://doi.org/10.1088/0004-637X/694/1/556)
- Blakeslee, J. P., Cantiello, M., Mei, S., et al. 2010, *ApJ*, 724, 657, doi: [10.1088/0004-637X/724/1/657](https://doi.org/10.1088/0004-637X/724/1/657)
- Brout, D., & Scolnic, D. 2021, *ApJ*, 909, 26, doi: [10.3847/1538-4357/abd69b](https://doi.org/10.3847/1538-4357/abd69b)
- Brout, D., Taylor, G., Scolnic, D., et al. 2022, *ApJ*, 938, 111, doi: [10.3847/1538-4357/ac8bcc](https://doi.org/10.3847/1538-4357/ac8bcc)
- Brown, P. J., Perry, J. M., Beeny, B. A., Milne, P. A., & Wang, X. 2018, *ApJ*, 867, 56, doi: [10.3847/1538-4357/aae1ad](https://doi.org/10.3847/1538-4357/aae1ad)
- Burns, C. R., Stritzinger, M., Phillips, M. M., et al. 2011, *AJ*, 141, 19, doi: [10.1088/0004-6256/141/1/19](https://doi.org/10.1088/0004-6256/141/1/19)
- Burns, C. R., Parent, E., Phillips, M. M., et al. 2018, *ApJ*, 869, 56, doi: [10.3847/1538-4357/aae51c](https://doi.org/10.3847/1538-4357/aae51c)
- Cantiello, M., Grado, A., Blakeslee, J. P., et al. 2013, *A&A*, 552, A106, doi: [10.1051/0004-6361/201220756](https://doi.org/10.1051/0004-6361/201220756)
- Cantiello, M., Blakeslee, J. P., Ferrarese, L., et al. 2018, *ApJ*, 856, 126, doi: [10.3847/1538-4357/aab043](https://doi.org/10.3847/1538-4357/aab043)
- Chen, R., Scolnic, D., Rozo, E., et al. 2022, *ApJ*, 938, 62, doi: [10.3847/1538-4357/ac8b82](https://doi.org/10.3847/1538-4357/ac8b82)
- Childress, M. J., Wolf, C., & Zahid, H. J. 2014, *MNRAS*, 445, 1898, doi: [10.1093/mnras/stu1892](https://doi.org/10.1093/mnras/stu1892)
- Efstathiou, G. 2021, *MNRAS*, 505, 3866, doi: [10.1093/mnras/stab1588](https://doi.org/10.1093/mnras/stab1588)
- Foley, R. J., Scolnic, D., Rest, A., et al. 2018, *MNRAS*, 475, 193, doi: [10.1093/mnras/stx3136](https://doi.org/10.1093/mnras/stx3136)
- Freedman, W. L., Madore, B. F., Gibson, B. K., et al. 2001, *ApJ*, 553, 47, doi: [10.1086/320638](https://doi.org/10.1086/320638)
- Freedman, W. L., Madore, B. F., Hatt, D., et al. 2019, *ApJ*, 882, 34, doi: [10.3847/1538-4357/ab2f73](https://doi.org/10.3847/1538-4357/ab2f73)
- Gall, C., Stritzinger, M. D., Ashall, C., et al. 2018, *A&A*, 611, A58, doi: [10.1051/0004-6361/201730886](https://doi.org/10.1051/0004-6361/201730886)
- Gallagher, J. S., Garnavich, P. M., Berlind, P., et al. 2005, *ApJ*, 634, 210, doi: [10.1086/491664](https://doi.org/10.1086/491664)
- Ganeshalingam, M., Li, W., Filippenko, A. V., et al. 2010, *ApJS*, 190, 418, doi: [10.1088/0067-0049/190/2/418](https://doi.org/10.1088/0067-0049/190/2/418)
- Garnavich, P. M., Jha, S., Challis, P., et al. 1998, *ApJ*, 509, 74, doi: [10.1086/306495](https://doi.org/10.1086/306495)
- Garnavich, P. M., Bonanos, A. Z., Krisciunas, K., et al. 2004, *ApJ*, 613, 1120, doi: [10.1086/422986](https://doi.org/10.1086/422986)
- Guy, J., Astier, P., Nobili, S., Regnault, N., & Pain, R. 2005, *A&A*, 443, 781, doi: [10.1051/0004-6361:20053025](https://doi.org/10.1051/0004-6361:20053025)
- Guy, J., Astier, P., Baumont, S., et al. 2007, *A&A*, 466, 11, doi: [10.1051/0004-6361:20066930](https://doi.org/10.1051/0004-6361:20066930)
- Hamuy, M., Cartier, R., Contreras, C., & Suntzeff, N. B. 2021, *MNRAS*, 500, 1095, doi: [10.1093/mnras/staa3350](https://doi.org/10.1093/mnras/staa3350)
- Hamuy, M., Phillips, M. M., Maza, J., et al. 1995, *AJ*, 109, 1, doi: [10.1086/117251](https://doi.org/10.1086/117251)

- Hamuy, M., Phillips, M. M., Suntzeff, N. B., et al. 1996, AJ, 112, 2391, doi: [10.1086/118190](https://doi.org/10.1086/118190)
- Hicken, M., Challis, P., Jha, S., et al. 2009, ApJ, 700, 331, doi: [10.1088/0004-637X/700/1/331](https://doi.org/10.1088/0004-637X/700/1/331)
- Hicken, M., Challis, P., Kirshner, R. P., et al. 2012, ApJS, 200, 12, doi: [10.1088/0067-0049/200/2/12](https://doi.org/10.1088/0067-0049/200/2/12)
- Hubble, E. 1929, Proceedings of the National Academy of Science, 15, 168, doi: [10.1073/pnas.15.3.168](https://doi.org/10.1073/pnas.15.3.168)
- Huchra, J. P. 1992, Science, 256, 321, doi: [10.1126/science.256.5055.321](https://doi.org/10.1126/science.256.5055.321)
- Jensen, J. B., Blakeslee, J. P., Gibson, Z., et al. 2015, ApJ, 808, 91, doi: [10.1088/0004-637X/808/1/91](https://doi.org/10.1088/0004-637X/808/1/91)
- Jensen, J. B., Tonry, J. L., Thompson, R. I., et al. 2001, ApJ, 550, 503, doi: [10.1086/319819](https://doi.org/10.1086/319819)
- Jensen, J. B., Blakeslee, J. P., Ma, C.-P., et al. 2021, ApJS, 255, 21, doi: [10.3847/1538-4365/ac01e7](https://doi.org/10.3847/1538-4365/ac01e7)
- Jha, S., Riess, A. G., & Kirshner, R. P. 2007, ApJ, 659, 122, doi: [10.1086/512054](https://doi.org/10.1086/512054)
- Jha, S., Kirshner, R. P., Challis, P., et al. 2006, AJ, 131, 527, doi: [10.1086/497989](https://doi.org/10.1086/497989)
- Kawabata, M., Maeda, K., Yamanaka, M., et al. 2020, ApJ, 893, 143, doi: [10.3847/1538-4357/ab8236](https://doi.org/10.3847/1538-4357/ab8236)
- Kelly, P. L., Hicken, M., Burke, D. L., Mandel, K. S., & Kirshner, R. P. 2010, ApJ, 715, 743, doi: [10.1088/0004-637X/715/2/743](https://doi.org/10.1088/0004-637X/715/2/743)
- Kelsey, L., Sullivan, M., Smith, M., et al. 2021, MNRAS, 501, 4861, doi: [10.1093/mnras/staa3924](https://doi.org/10.1093/mnras/staa3924)
- Kessler, R., Bernstein, J. P., Cinabro, D., et al. 2009, PASP, 121, 1028, doi: [10.1086/605984](https://doi.org/10.1086/605984)
- Khetan, N., Izzo, L., Branchesi, M., et al. 2021, A&A, 647, A72, doi: [10.1051/0004-6361/202039196](https://doi.org/10.1051/0004-6361/202039196)
- Lampeitl, H., Smith, M., Nichol, R. C., et al. 2010, ApJ, 722, 566, doi: [10.1088/0004-637X/722/1/566](https://doi.org/10.1088/0004-637X/722/1/566)
- Lemaître, G. 1927, Annales de la Societ e Scientifique de Bruxelles, 47, 49
- Ma, C.-P., Greene, J. E., McConnell, N., et al. 2014, ApJ, 795, 158, doi: [10.1088/0004-637X/795/2/158](https://doi.org/10.1088/0004-637X/795/2/158)
- Mosher, J., Guy, J., Kessler, R., et al. 2014, ApJ, 793, 16, doi: [10.1088/0004-637X/793/1/16](https://doi.org/10.1088/0004-637X/793/1/16)
- Perlmutter, S., Aldering, G., della Valle, M., et al. 1998, Nature, 391, 51, doi: [10.1038/34124](https://doi.org/10.1038/34124)
- Perlmutter, S., Aldering, G., Goldhaber, G., et al. 1999, ApJ, 517, 565, doi: [10.1086/307221](https://doi.org/10.1086/307221)
- Phillips, M. M. 1993, ApJL, 413, L105, doi: [10.1086/186970](https://doi.org/10.1086/186970)
- Phillips, M. M., Lira, P., Suntzeff, N. B., et al. 1999, AJ, 118, 1766, doi: [10.1086/301032](https://doi.org/10.1086/301032)
- Pietrzyński, G., Graczyk, D., Gellenne, A., et al. 2019, Nature, 567, 200, doi: [10.1038/s41586-019-0999-4](https://doi.org/10.1038/s41586-019-0999-4)
- Planck Collaboration, Aghanim, N., Akrami, Y., et al. 2020, A&A, 641, A6, doi: [10.1051/0004-6361/201833910](https://doi.org/10.1051/0004-6361/201833910)
- Pruzhinskaya, M. V., Novinskaya, A. K., Pauna, N., & Rosnet, P. 2020, MNRAS, 499, 5121, doi: [10.1093/mnras/staa3173](https://doi.org/10.1093/mnras/staa3173)
- Riess, A. G., Casertano, S., Yuan, W., Macri, L. M., & Scolnic, D. 2019, ApJ, 876, 85, doi: [10.3847/1538-4357/ab1422](https://doi.org/10.3847/1538-4357/ab1422)
- Riess, A. G., Press, W. H., & Kirshner, R. P. 1996, ApJ, 473, 88, doi: [10.1086/178129](https://doi.org/10.1086/178129)
- Riess, A. G., Filippenko, A. V., Challis, P., et al. 1998, AJ, 116, 1009, doi: [10.1086/300499](https://doi.org/10.1086/300499)
- Riess, A. G., Kirshner, R. P., Schmidt, B. P., et al. 1999, AJ, 117, 707, doi: [10.1086/300738](https://doi.org/10.1086/300738)
- Riess, A. G., Macri, L., Casertano, S., et al. 2009, ApJ, 699, 539, doi: [10.1088/0004-637X/699/1/539](https://doi.org/10.1088/0004-637X/699/1/539)
- Riess, A. G., Macri, L. M., Hoffmann, S. L., et al. 2016, ApJ, 826, 56, doi: [10.3847/0004-637X/826/1/56](https://doi.org/10.3847/0004-637X/826/1/56)
- Riess, A. G., Yuan, W., Macri, L. M., et al. 2022, ApJL, 934, L7, doi: [10.3847/2041-8213/ac5c5b](https://doi.org/10.3847/2041-8213/ac5c5b)
- Rose, B. M., Garnavich, P. M., & Berg, M. A. 2019, ApJ, 874, 32, doi: [10.3847/1538-4357/ab0704](https://doi.org/10.3847/1538-4357/ab0704)
- Scannapieco, E., & Bildsten, L. 2005, ApJL, 629, L85, doi: [10.1086/452632](https://doi.org/10.1086/452632)
- Scolnic, D., Smith, M., Massiah, A., et al. 2020, ApJL, 896, L13, doi: [10.3847/2041-8213/ab8735](https://doi.org/10.3847/2041-8213/ab8735)
- Scolnic, D., Brout, D., Carr, A., et al. 2022, ApJ, 938, 113, doi: [10.3847/1538-4357/ac8b7a](https://doi.org/10.3847/1538-4357/ac8b7a)
- Sullivan, M., Le Borgne, D., Pritchett, C. J., et al. 2006, ApJ, 648, 868, doi: [10.1086/506137](https://doi.org/10.1086/506137)
- Sullivan, M., Conley, A., Howell, D. A., et al. 2010, MNRAS, 406, 782, doi: [10.1111/j.1365-2966.2010.16731.x](https://doi.org/10.1111/j.1365-2966.2010.16731.x)
- Taylor, G., Lidman, C., Tucker, B. E., et al. 2021, MNRAS, 504, 4111, doi: [10.1093/mnras/stab962](https://doi.org/10.1093/mnras/stab962)
- Tonry, J., & Schneider, D. P. 1988, AJ, 96, 807, doi: [10.1086/114847](https://doi.org/10.1086/114847)
- Tripp, R. 1998, A&A, 331, 815